# Fivefold compression of 250-TW laser pulses

Vladislav Ginzburg,[1,*] Ivan Yakovlev,[1] Alexandr Zuev,[1] Anastasia Korobeynikova,[1] Anton Kochetkov,[1] Alexey Kuzmin,[1] Sergey Mironov,[1] Andrey Shaykin,[1] Ilya Shaikin,[1] Efim Khazanov,[1] and Gerard Mourou[2]

[1]*Institute of Applied Physics of the Russian Academy of Sciences, Nizhny Novgorod, Russia*

[2]*International Center for Zetta-Exawatt Science and Technology, Palaiseau, France*

(Received 12 July 2019; published 27 January 2020)

The pulse spectrum at the laser output was broadened due to self-phase modulation in fused silica and then the pulse was compressed by chirped mirrors. It was demonstrated that with an optimal choice of mirror dispersion a pulse with an energy of 17 J can be compressed from 70 to 14 fs. This compression after compressor approach has undoubted merits: simplicity, low cost, negligible pulse energy losses, and applicability to any high-power laser.

DOI: 10.1103/PhysRevA.101.013829

## I. INTRODUCTION

In just a few years of their existence, lasers reached an intensity of $10^{14}$ W/cm$^2$. However, for the next 20 years, the intensity practically did not grow. The reason for this plateau was that the laser amplifiers reached their limits stipulated by the optical breakdown threshold of laser media. In 1985 [1] chirped pulse amplification (CPA) was proposed. Now almost all high-power lasers use CPA: a stretcher on diffraction gratings with positive dispersion, amplifier, and compressor on diffraction gratings with negative dispersion [see Fig. 1(a)]. For CPA, it is fundamentally important that, when a pulse is compressed, its energy does not increase, i.e., compression can be done without pulse propagation in the medium, using only reflective optical elements—diffraction gratings. The discovery of CPA led to a dramatic laser power enhancement; by the beginning of the 2000s, the record intensity reached $10^{22}$ W/cm$^2$ [2]. After that, however, the intensity almost did not grow—there appeared a second plateau. The reason for this was that in the early 2000s the power (and intensity) increased so much that it was no longer limited by the fact that the laser pulse could not be further amplified, but that it could not be compressed. The diffraction gratings damage threshold limits the intensity at the laser output. Thus, the compressor is now the weakest link in the stretcher-amplifier-compressor chain.

What next? The enhancement of laser power and intensity is possible in two ways. First, it is the creation of a mosaic compressor or of phase-locked parallel CPA channels, each having its own compressor at the output. This pathway has a number of significant drawbacks: technical and technological difficulties, the need for a multiple pulse energy increase, as well as the size and price of the laser. We prefer the second, much simpler and cheaper way: an increase in power not due to an increase in energy, but due to a decrease in pulse duration [3–5]. This method is called thin-film compression, thin plate compression, or the compression after compressor approach (CafCA). The idea is as follows [see Fig. 1(b)].

The pulse duration at the CPA output is usually a little more than the Fourier limit, so for substantial shortening it is necessary to increase the width of the spectrum, i.e., stretch the pulse spectrum rather than its duration as in CPA. The simplest and most suitable way is to use self-phase modulation (SPM) in a Kerr-nonlinear medium, the refractive index of which, $n$, depends on pulse intensity $I$: $n = n_0 + n_2 I$, where $n_0$ is the linear index of refraction and $n_2$ is the nonlinear index of refraction. At the output of the medium, the pulse is positively chirped. Chirped mirrors (CMs) induce the negative chirp of the same absolute value, just like the compressor does in CPA (see Fig. 1). As a result, the pulse is shortened and the laser power is increased.

As shown in [6], the intensity increase factor $F_i = I_{out}/I_{in}$ at small linear dispersion may be estimated as

$$F_i = 1 + B/2, \tag{1}$$

where $B = kLn_2I$ is called a break-up integral or the $B$ integral, $k = 2\pi/\lambda$, $L$ is the length of the nonlinear medium, and $\lambda$ is the central wavelength in vacuum.

The idea to use SPM for pulse compression was put forth in 1969 in [7], and the same year several-fold compression of a 20-ps pulse in a $CS_2$-filled cuvette was demonstrated in [8]. Later the SPM was implemented in the femtosecond range in a fiber [9], in gas filled hollow waveguides [10], and in solid state with restricted propagation [11]. However, in all further experiments (see the detailed review [12]) the pulse power was below 30 GW as the beam diameter was less than 1 mm. Evidently, power scaling is possible only with free propagation in a bulk nonlinear medium.

## II. OVERCOMING CafCA LIMITATIONS FOR TW AND PW PULSES

There are three problems that impede the implementation of CafCA for a free-propagating laser beam.

The first group of problems is associated with the nonuniform intensity distribution of the beam: self-focusing of the beam as a whole, phase aberrations, and, most importantly, nonuniform temporal pulse compression across the beam.

*vlgin@rambler.ru

 

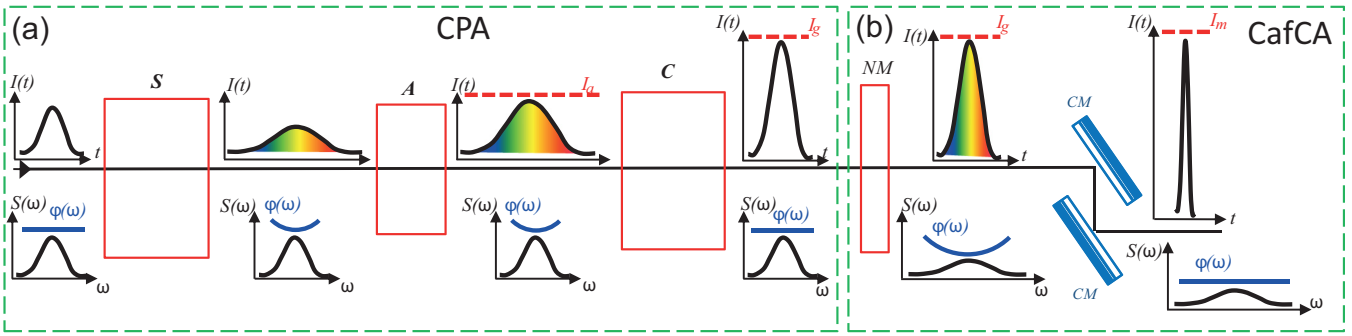


FIG. 1. The idea of CPA (a) and CafCA (b). S, stretcher; A, laser amplifier; C, compressor; NM, nonlinear medium; CM, chirped mirror; $I_a$, $I_g$, and $I_m$, breakdown threshold of the amplifiers, diffraction gratings, and chirped mirrors, respectively.

Using a negative lens as a nonlinear medium as a solution to these problems was proposed in [4] and then implemented experimentally in [13,14], which immediately brought the CafCA from the multi-GW to the TW range.

Another problem is appearance of small-scale self-focusing (SSSF) induced by the Bespalov-Talanov instability [15]. The instability increment is determined by the $B$ integral. Usually, at $B = 3$ the beam breaks up into multiple filaments. At the same time, as seen from (1), at $B < 3$ only a 2.5-fold power enhancement is possible. Thus, a significant increase in power using CafCA seems impracticable at first sight: one and the same effect (cubic nonlinearity) and, moreover, the same parameter ($B$ integral) are both useful and parasitic. Consequently, until recently it was believed that CafCA is possible only in a narrow $2 < B < 3$ range [3,16–19]. A fundamentally important feature of SSSF in ultra-high-power femtosecond lasers as compared to nanosecond lasers is a significant expansion of the angular instability range. This occurs because the optical element damage threshold in the femtosecond range is much higher, and the laser radiation intensity is in units of $\mathrm{TW/cm^2}$ rather than units of $\mathrm{GW/cm^2}$. The most dangerous angle $\theta_{\max}$ (angle of propagation of spatial noise with the largest instability increment) is proportional to the root of the intensity and, hence, increases by a factor of 30 and amounts to tens of mrad. The solution of SSSF suppression for ultra-high-power lasers proposed in [20] is based on using self-filtering of the beam freely propagating in vacuum—the most dangerous noise components ($\theta$ on the order of $\theta_{\max}$) come out of the beam aperture (Fig. 2). It is obvious that self-filtering is efficient if the angle of vision $\theta_v = R/L_f$ (where $R$ is the beam radius) is approximately

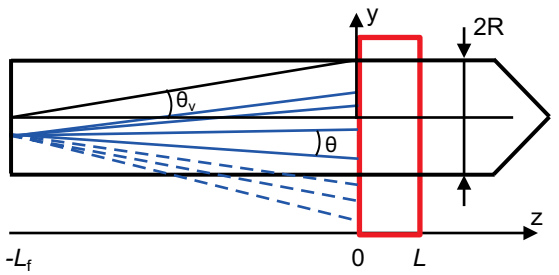


FIG. 2. Beam self-filtering during propagation in free space: part of the noise (the rays are shown by dashed lines) goes beyond the beam aperture on propagating distance $L_f$.

equal to $\theta_{\max}$ or less. For nanosecond lasers with intensity on the order of $\mathrm{GW/cm^2}$, $\theta_{\max}$ is equal approximately to 1 mrad and self-filtering is possible only at a very large distance $L_f$. For femtosecond lasers with $\mathrm{TW/cm^2}$ intensity, $\theta_{\max}$ is much larger, which leads to practicably feasible distances $L_f$.

In other words, free space is a filter of spatial frequencies, the transmission coefficient of which $T$ can be estimated as follows. Consider an arbitrary point of the beam cross section $(r,\varphi)$ in the $z = -L_f$ plane from which "noise" rays are propagating at an angle $\theta$ to the $z$ axis. In the $z = 0$ plane, part of these rays will be incident on the beam aperture (solid curves in Fig. 2), and part of the rays will go beyond the aperture (dashed lines in Fig. 2). Consider that the part of the rays incident on the aperture is the noise transmittance $t$. By integrating $t$ with respect to the cross section, we can readily obtain an expression for $T$:

$$T\left(\frac{\theta}{\theta_v}\right) = \frac{1}{\pi}\int_0^1 \mathrm{Re}\left\{\arccos\left[\frac{(\theta/\theta_v)^2 + y - 1}{2\sqrt{y}\theta/\theta_v}\right]\right\} dy. \quad (2)$$

Numerical simulation with diffraction taken into account showed that this formula is highly accurate. In [5,21,22] it was demonstrated that self-filtering mitigates the once inviolable limitation $B < 3$.

The third problem is technological—a very large aspect ratio of the nonlinear medium, which is especially acute for petawatt powers. It is caused by the need for higher peak power of the laser pulse, larger beam diameter, and a thinner nonlinear medium. The idea of using polymer materials [23] promoted the solution of this problem significantly. The linear and nonlinear optical properties of polymer materials are currently actively investigated and the results are highly promising. In particular, a 2.6-fold compression of a pulse with a power of 100 TW was obtained with the use of polyethylene terephthalate [24].

Over the last years several successful experiments with CafCA were performed with pulse power from 1 to 200 TW [5,6,24–26] with up to a threefold compression factor. In this paper we report the next step: fivefold pulse compression has been demonstrated in experiments at $B = 7.5$.

## III. EXPERIMENTAL RESULTS

The schematic diagram of the experiment is presented in Fig. 3. The beam of the laser PEARL (central wavelength

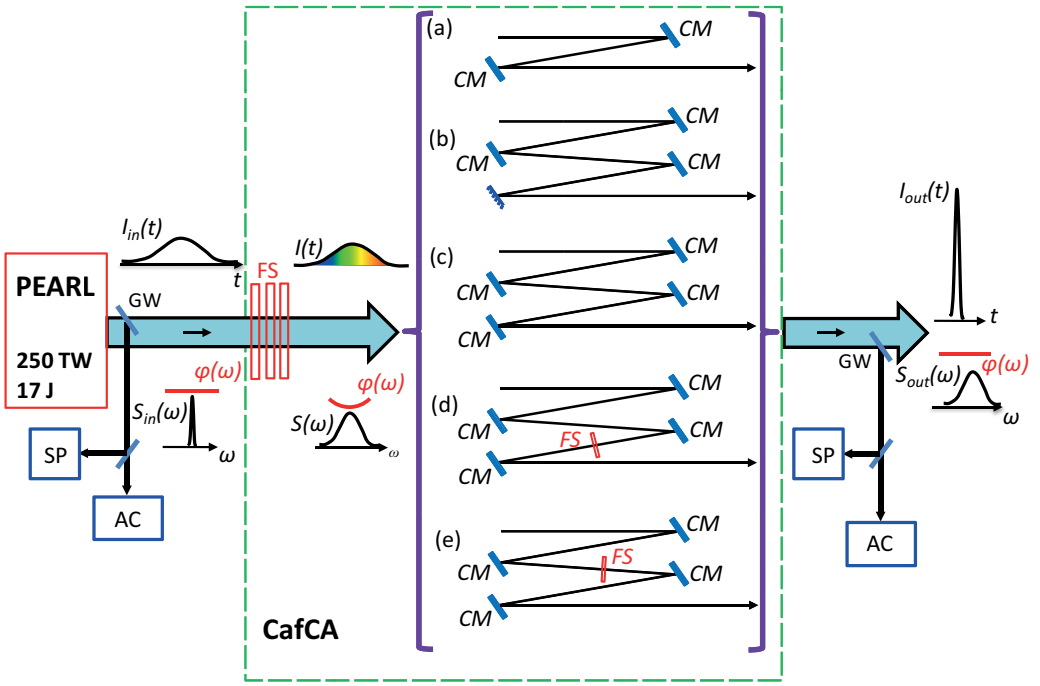


FIG. 3. Schematic diagram of the experiment. FS, fused silica plates; CM, chirped mirrors; GW, small-aperture glass wedges; AC, autocorrelators; SP, spectrometers.

910 nm, pulse duration 65–75 fs, pulse energy up to 17 J, diameter 18 cm) was reflected at the final diffraction grating of the compressor and propagated 2.5 m in free space for self-filtering. After that the beam successively passed through three 1-mm-thick fused silica plates spaced apart by about 1 cm. The use of three plates instead of a single 3-mm plate allows decreasing the SSSF [12]. Further, after reflection at the 45° mirror and free propagation over a distance of 4 m the beam arrived at the system of CMs. Part (∼0.2%) of the radiation that had passed through the 45° mirror was extracted from the compressor and used for recording the beam cross section. Each chirped mirror (UltraFast Innovations GmbH) had dispersion $\alpha_1 = -100\,\mathrm{fs}^2$ and reflectivity 99.5% in 810–1010-nm bandwidth. Five variants of CafCA were investigated: three single-stage versions with two, three, and four mirrors, and two two-stage [23] versions with 3+1 and 2+2 mirrors, as shown in Figs. 3(a)–3(e), respectively. In all variants the first two CMs were 20 cm in diameter and other CMs were 5 cm in diameter. So in the last four variants only the central part of the beam with 5-cm diameter was compressed.

For measuring the parameters of the input and output pulses, two glass wedges with an aperture of 1×2 cm and a mat back surface were placed on the beam path: one at

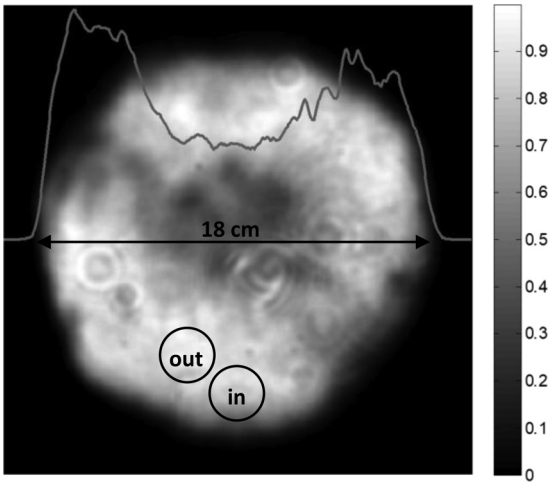


FIG. 4. Output PEARL laser beam intensity in the near field. The circles mark the sites of measuring the input and output spectra and ACF.

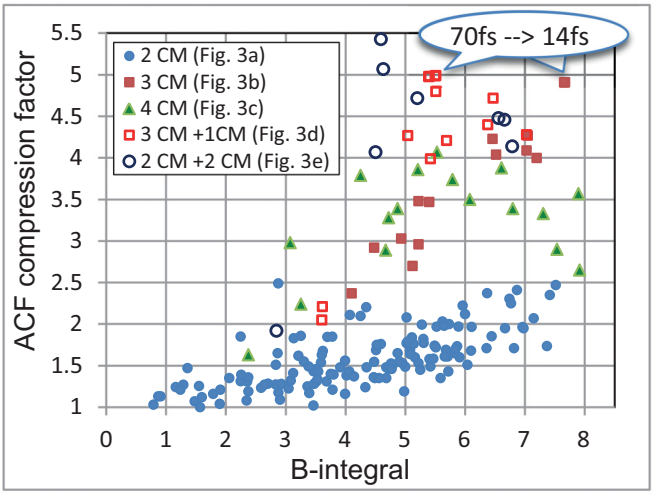


FIG. 5. Compression factor $F_{\mathrm{ACF}}$ vs the B integral for five variants of CafCA shown in Figs. 3(a)–3(e).

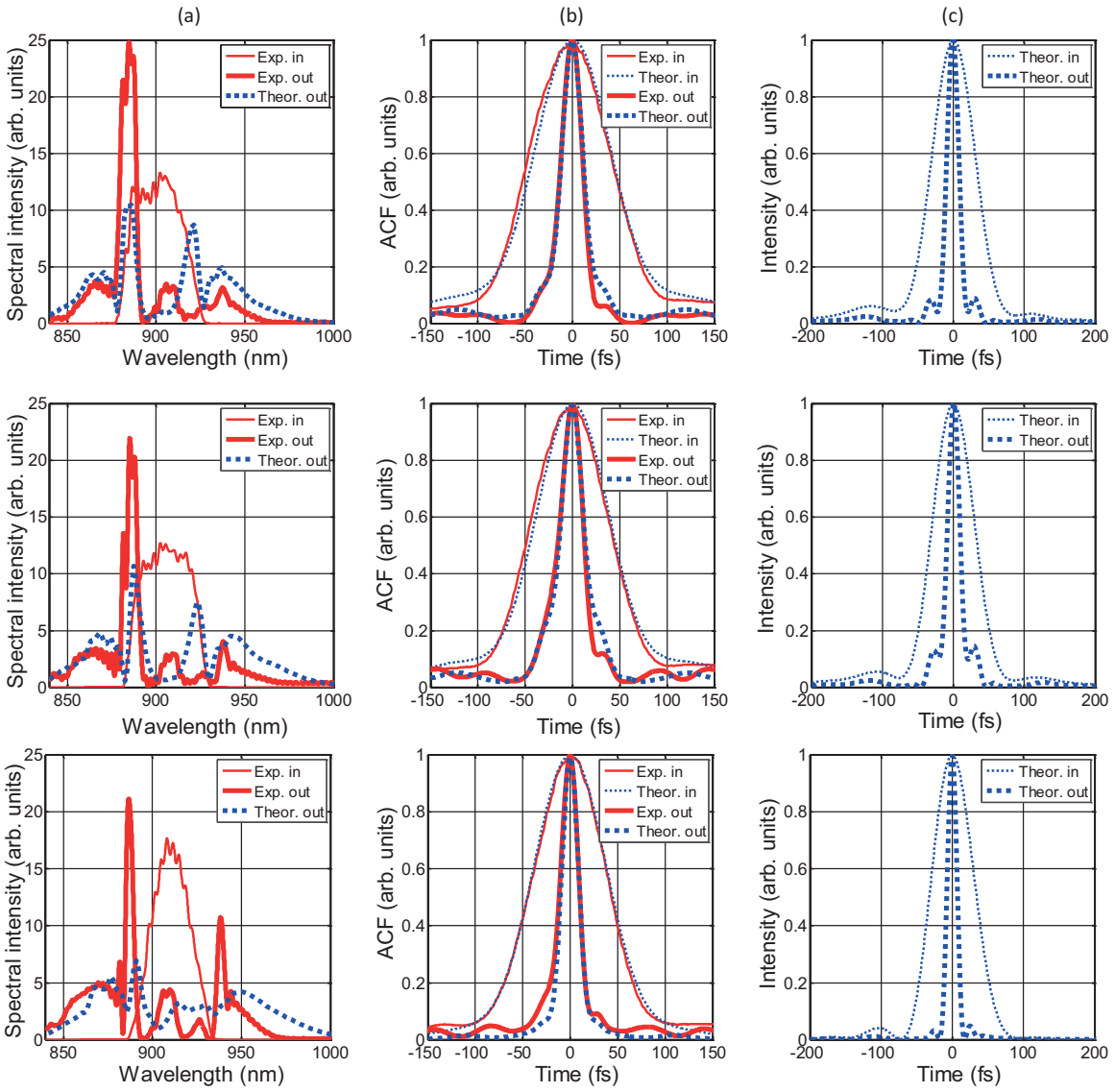


FIG. 6. (a) Spectra, (b) ACFs, and (c) shapes of three different pulses at the input (thin curves) and output (bold curves) of the CafCA system: experimental (solid red curves) and theoretical (dotted blue curves). Parameters of these three pulses are shown in Table I.

the PEARL output, and the other at the CafCA output. On reflection from the wedges the beams were directed to two spectrometers and two autocorrelators. The intensity distribution in the beam at the PEARL laser output, as well as the sites of measuring the input and output spectra and the autocorrelation function (ACF), are shown in Fig. 4. As the beam in the region of measurements was quite homogeneous, without fused silica plates the spectra and durations of the input and output pulses coincided to an accuracy up to 10%. For pulses having a duration of 65–75 fs, the dispersion introduced by the chirped mirrors did not appreciably increase the duration. Thus, the radiation characteristics were measured in one "shot."

The dependence of the compression factor $F_{ACF}$—the ratio of the full width at half maximum duration of intensity ACF of the pulse at the CafCA input and output—on the $B$ integral was measured for all five CafCA variants shown in Fig. 3. The results of the measurements for a single-stage CafCA [Figs. 3(a)–3(c)] and two-stage CafCA [Figs. 3(d) and 3(e)] are presented in Fig. 5. As is seen from Fig. 5, the dispersion of two chirped mirrors is insufficient. For moderate values of the $B$ integral ($B < 6$), the variant with four mirrors is optimal, and for the maximum values of the $B$ integral ($B > 6$) the optimal variant is with three mirrors. This is in a qualitative agreement with the theory [12] for Fourier-transform limited (FTL) Gaussian pulses at the CafCA input, according to which the higher the $B$ integral the lower the optimal value of CM dispersion that is needed. In our experiments, the pulse at the CafCA input was neither Gaussian nor FTL. Its shape and duration slightly varied from pulse to pulse. The spectra, ACFs, and pulse shapes for the three different pulses are presented in Fig. 6. The solid red lines correspond to the experimental data. Based on the measured spectra, we chose the pulse shapes the ACFs of which were closest to the measured ACFs. Their shapes and ACFs are shown by the blue dotted lines in Fig. 6.

TABLE I. Parameters of the three shots shown in Fig. 6.

| CafCA variant | $B$ | $F_{\mathrm{ACF,exp}}$ | $F_{\mathrm{ACF,th}}$ | $F_{\mathrm{pulse}}$ | $F_{\mathrm{i}}$ | $T_{\mathrm{in}}$ (fs) | $T_{\mathrm{out}}$(fs) |
|---|---|---|---|---|---|---|---|
| Fig. 3(b) | 7 | 4.1 | 4.4 | 4.3 | 4.1 | 67 | 15.5 |
| Fig. 3(c) | 6.8 | 3.9 | 3.8 | 3.5 | 3.1 | 70 | 20 |
| Fig. 3(c) | 7.3 | 3.4 | 3.3 | 3.4 | 2.8 | 67 | 20 |

For the input pulses obtained in this way, we calculated the dynamics of their propagation in a nonlinear medium (in fused silica plates). The calculations took into account cubic nonlinearity ($n_2 = 3\times10^{-16}\,\mathrm{cm}^2/\mathrm{W}$) and dispersion ($k_2 = 28\,\mathrm{fs}^2/\mathrm{mm}$). A quadratic phase introduced by CMs ($-100\,\mathrm{fs}^2$ per mirror) was added to the pulse spectrum at the output of the nonlinear medium. The results of the calculations are shown in Fig. 6 by bold dotted lines.

Significant spectrum broadening at the CafCA output [compare the bold and thin solid lines in Fig. 6(a)], as well as the emergence of narrow peaks instead of a smooth modulation typical of FTL pulses after SPM, are clearly seen in Fig. 6. These peaks arise because the pulses at the CafCA input are not FTL. This effect was discussed in detail in [6]. The theoretical and experimental spectra at the CafCA output agree qualitatively, although the peak widths and amplitudes differ quantitatively [compare the bold solid and dotted curves in Fig. 6(a)].

Comparison of the theoretical and experimental ACF of the output (compensated) pulses also gives a good agreement [see Fig. 6(b)]. For the three shots shown in Fig. 6, the experimental ACF compression factor $F_{\mathrm{ACF,exp}}$ is very close to the theoretical factor $F_{\mathrm{ACF,th}}$ and to the pulse duration shortening $F_{\mathrm{pulse}} = T_{\mathrm{in}}/T_{\mathrm{out}}$ (see Table I). As the compressed pulses are not Gaussian, their intensity increase factor $F_{\mathrm{i}} = I_{\mathrm{out}}/I_{\mathrm{in}}$ is not equal to $F_{\mathrm{pulse}}$. As seen from Table I for these three shots $F_{\mathrm{i}}$ is smaller than $F_{\mathrm{pulse}}$ but the difference is not crucial. This is in good agreement with the detailed theoretical study [12], where it was shown that $F_{\mathrm{i}}$ is typically smaller than $F_{\mathrm{pulse}}$ by 10–20% only. Other shots also showed good coincidence experimental data with theory. As is seen from Fig. 5 the highest compression factor $F_{\mathrm{ACF,exp}}$ is about 5 (the 70-fs pulse is compressed to a 14-fs pulse).

Note that, despite the extremely large values of the $B$ integral (about 8), thanks to the self-filtering, optical breakdown was not observed either in the fused silica plates used for SPM or in the CMs. Absence of SSSF is also confirmed by the fact that there were no distortions typical for SSSF in the near field of the beam that was measured after the nonlinear plates. The near field (Fig. 4) remained almost unchanged when the plates had been removed from the beam aperture. The detailed numerical simulation made in [27] showed that, when a beam with an intensity of $11\,\mathrm{TW/cm}^2$ is propagating in a nonlinear medium, first the intensity increases substantially due to SSSF, and then photoionization, impact ionization, and ionization-induced optical nonlinearity take place. This is attributed to a high, of order 9 eV, band-gap value. In our experiments the intensity was even lower—of the order of $1\,\mathrm{TW/cm}^2$, therefore the absence of SSSF implies that no plasma was formed inside the nonlinear element.

As mentioned above, CafCA works well for beams with a homogeneous near-field intensity distribution typical for high-power lasers. In our experiments, the intensity distribution in the near field had 50% modulation (Fig. 4). After propagation in a nonlinear medium, the beam phase also acquires a strong inhomogeneity (in a first approximation, the nonlinear phase incursion is proportional to intensity), and this inhomogeneity is unsteady in time. This leads to less efficient focusing, i.e., to a decrease in the Strehl ratio at the pulse maximum. This parasitic effect can be eliminated by means of an adaptive mirror which introduces into the beam a phase the absolute value of which is equal to that of the phase at the pulse maximum after compression by the chirped mirrors but has an opposite sign. The potential of the commercially available adaptive mirrors is as a rule restricted to Zernicke polynomials with indices below 10. Therefore, full suppression (Strehl ratio equal to 1) cannot be attained. We performed three-dimensional simulation of the SPM process (taking into account material dispersion), of compression on chirped mirrors, and of phase compensation by an adaptive mirror for the input radiation with experimentally measured spatial (Fig. 4) and close to the experimental temporal shapes (Fig. 6). The results demonstrated that a set of Zernicke polynomials with radial indices not more than 7 is sufficient for the Strehl ratio to reach 0.85. Thus, the focusing will be efficient even for beams with strongly inhomogeneous distribution. Note that the lowest Zernicke polynomial (defocus) leads only to a moving focal plane and may be "compensated" by moving a target without an adaptive mirror. This "compensation" could be efficient for bell shaped beams.

We also studied two-stage CafCA [Figs. 3(d) and 3(e)]. The experimental results are shown by the empty symbols in Fig. 5, where the $B$ integral at the first stage is plotted along the horizontal axis. The addition of the second stage with three mirrors in the first one [Fig. 3(d)] resulted in an insignificant increase of the CafCA efficiency (cf. the empty and filled squares in Fig. 5). The operation of the second CafCA stage is demonstrated best with the use of two mirrors at the first stage [Fig. 3(e); cf. the empty and filled circles in Fig. 5]. Note that in both two-stage variants the compressed pulse duration was measured to be 14–15 fs, which is, probably, a limiting resolution of the used diagnostics. A detailed study of the two-stage CafCA will be given in a separate publication.

The demonstrated fivefold compression of 250-TW pulses indicates that there are no technological limitations on using the CafCA method for lasers with a power level of 1 PW and above. The output power enhancement up to 1 PW will increase the intensity by a factor of 4, which will demand a fourfold shortening of the nonlinear medium (from 3 to 0.75 mm). Lasers with a power of several PW have a larger beam aperture but approximately the same intensity of a few $\mathrm{TW/cm}^2$. Additionally, 0.1-mm-thick plastic films successfully used in [28] almost fully lift fabrication limitations.

## IV. CONCLUSION

The results presented here demonstrate that fivefold shortening (from 70 to 14 fs) of a 250-TW pulse can be attained by means of nonlinear compression. The efficiency of two-stage compression has been demonstrated. The CafCA has three principal merits. First, it offers simplicity and low cost: only a plane parallel plate and chirped mirrors, the fabrication

technique of which is well developed, are needed. Second, it offers high efficiency: energy loss, taking into account the possibility of placing a plate at a Brewster angle, does not exceed 1%. Third, almost all ultra-high-power lasers may be upgraded without any modification inside the laser.

It is expected that CafCA will find a wide application in the near future in petawatt and multipetawatt lasers, including lasers with a pulse duration of 15–25 fs, as well as with a duration of hundreds of femtoseconds, at the kJ energy level [27,29].


## ACKNOWLEDGMENTS

The work, including all experiments on single-stage compression, theoretical investigation and experimental data processing, was supported by the Ministry of Science and Higher Education of the Russian Federation, state assignment for the Institute of Applied Physics RAS, Project No. 0035-2020-0015. For diagnosing the radiation parameters after the second stage as well as for the experiments on two-stage compression, funds from the Russian Foundation for Basic Research (RFBR), Project No. 18-02-00850 a were also used.



[1] D. Strickland and G. Mourou, Opt. Commun. **56**, 219 (1985).

[2] S.-W. Bahk, P. Rousseau, T. A. Planchon, V. Chvykov, G. Kalintchenko, A. Maksimchuk, G. A. Mourou, and V. Yanovsky, Opt. Lett. **29**, 2837 (2004).

[3] G. Mourou, G. Cheriaux, and C. Radier, US Patent No. 20110299152 A1 (2009).

[4] S. Y. Mironov, V. V. Lozhkarev, E. A. Khazanov, and G. Mourou, Quantum Electron. **43**, 711 (2013).

[5] V. N. Ginzburg, I. V. Yakovlev, A. S. Zuev, A. A. Korobeynikova, A. A. Kochetkov, A. A. Kuz'min, S. Y. Mironov, A. A. Shaykin, I. A. Shaykin, and A. E. Khazanov, Quantum Electron. **49**, 299 (2019).

[6] V. N. Ginzburg, A. A. Kochetkov, I. V. Yakovlev, S. Y. Mironov, A. A. Shaykin, and E. A. Khazanov, Quantum Electron. **46**, 106 (2016).

[7] R. A. Fisher, P. L. Kelley, and T. K. Gustajson, Appl. Phys. Lett. **14**, 140 (1969).

[8] A. Laubereau, Phys. Lett. A **29**, 539 (1969).

[9] C. V. Shank, R. L. Fork, R. Yen, R. H. Stolen, and W. J. Tomlinson, Appl. Phys. Lett. **40**, 761 (1982).

[10] M. Nisoli, S. D. Silvestri, and O. Svelto, Appl. Phys. Lett. **68**, 2793 (1996).

[11] C. Rolland and P. B. Corkum, J. Opt. Soc. of Am. B **5**, 641 (1988).

[12] E. A. Khazanov, S. Y. Mironov, and G. Mourou, Phys. Usp. **62**, 038564 (2019).

[13] P. Lassonde, S. Mironov, S. Fourmaux, S. Payeur, E. Khazanov, A. Sergeev, J.-C. Kieffer, and G. Mourou, Laser Phys. Lett. **13**, 075401 (2016).

[14] S. Mironov, P. Lassonde, J. C. Kieffer, E. Khazanov, and G. Mourou, Eur. Phys. J. Spec. Top. **223**, 1175 (2014).

[15] V. I. Bespalov and V. I. Talanov, JETP Lett. **3**, 307 (1966).

[16] S. N. Vlasov, E. V. Koposova, and V. E. Yashin, Quantum Electron. **42**, 989 (2012).

[17] A. A. Mak, A. A. Andreev, and V. E. Yashin, Quantum Electron. **27**, 95 (1997).

[18] A. A. Mak and V. E. Yashin, Opt. Spectrosc. **70**, 1 (1991).

[19] N. V. Vysotina, N. N. Rosanov, and V. E. Yashin, Opt. Spectrosc. **110**, 973 (2011).

[20] S. Y. Mironov, V. V. Lozhkarev, V. N. Ginzburg, I. V. Yakovlev, G. Luchinin, A. A. Shaykin, E. A. Khazanov, A. A. Babin, E. Novikov, S. Fadeev, A. M. Sergeev, and G. A. Mourou, IEEE J. Sel. Topics Quantum Electron. **18**, 7 (2010).

[21] S. Mironov, V. Lozhkarev, G. Luchinin, A. Shaykin, and E. Khazanov, Appl. Phys. B: Lasers and Optics **113**, 147 (2013).

[22] V. N. Ginzburg, A. A. Kochetkov, A. K. Potemkin, and E. A. Khazanov, Quantum Electron. **48**, 325 (2018).

[23] G. Mourou, S. Mironov, E. Khazanov, and A. Sergeev, Eur. Phys. J. Spec. Top. **223**, 1181 (2014).

[24] S. Y. Mironov, V. N. Ginzburg, I. V. Yakovlev, A. A. Kochetkov, A. A. Shaykin, E. A. Khazanov, and G. A. Mourou, Quantum Electron. **47**, 614 (2017).

[25] D. M. Farinella, J. Wheeler, A. E. Hussein, J. Nees, M. Stanfield, N. Beier, Y. Ma, G. Cojocaru, R. Ungureanu, M. Pittman, J. Demailly, E. Baynard, R. Fabbri, M. Masruri, R. Secareanu, A. Naziru, R. Dabu, A. Maksimchuk, K. Krushelnick, D. Ros, G. Mourou, T. Tajima, and F. Dollar, J. Opt. Soc. Am B **36**, A28 (2019).

[26] S. Mironov, E. Gacheva, V. Ginzburg, D. E. Silin, A. Kochetkov, Y. Mamaev, A. Shaykin, E. Khazanov, and G. Mourou, Laser Phys. Lett. **12**, 025301 (2015).

[27] A. A. Voronin, A. M. Zheltikov, T. Ditmire, B. Rus, and G. Korn, Opt. Commun. **291**, 299 (2013).

[28] M. Masruri, J. Wheeler, I. Dancus, R. Fabbri, A. Nazîru, R. Secareanu, D. Ursescu, G. Cojocaru, R. Ungureanu, D. Farinella, M. Pittman, S. Mironov, S. Balascuta, D. Doria, D. Ros, and R. Dabu, in *Conference on Lasers and Electro-Optics*, OSA Technical Digest (Optical Society of America, Washington, DC, 2019), paper SW4E.3.

[29] S. Y. Mironov, J. Wheeler, R. Gonin, G. Cojocaru, R. Ungureanu, R. Banici, M. Serbanescu, R. Dabu, G. Mourou, and E. A. Khazanov, Quantum Electron. **47**, 173 (2017).